Edinburgh Research Explorer

Beam on beam control: beyond the particle approximation

OPEN ACCESS

Beam on beam control: beyond the particle approximation

Noel F. Smyth

School of Mathematics, University of Edinburgh, Edinburgh EH9 3FD, Scotland, U.K.
n.smyth@ed.ac.uk

Bryan Tope

School of Mathematics, University of Edinburgh, Edinburgh EH9 3FD, Scotland, U.K.
B.K.Tope@sms.ed.ac.uk

The all-optical control of the trajectory of a nonlinear optical beam propagating in a nematic liquid crystal cell is studied using a combination of modulation theory and full numerical solutions of the governing nematic equations. In detail, the output position of a signal beam is controlled via its interaction with a second, co-propagating control beam. The input positions of both the signal and control beams are fixed, with the output position of the signal beam determined by the input angle of the control beam. A simple modulation theory based on treating the optical beams as mechanical particles in a potential well is found to give only adequate agreement with numerical solutions. However, extending this modulation theory to include the detailed profiles of the beams, so that the beams are treated as rigid bodies moving in a potential well, leads to simple, extended equations which determine the input angle of the control beam required for a given output position of the signal beam. The predictions of this extended particle theory, or rigid body theory, are compared with full numerical solutions of the nematic equations and excellent agreement is found.

Keywords: nonlinear optics, liquid crystals, solitary waves, modulation theory

1. Introduction

Nematic liquid crystals have proved to be an ideal medium in which to study many nonlinear optical phenomena due to their "huge" nonlinear response, which enables nonlinear effects to be observed over millimetre distances[1,2]. Nematic liquid crystals having a focusing response to optical beams, so that the refractive index increases with the beam intensity[1], leading to self-sustaining beams for which this self-focusing balances linear diffraction[1,3]. Nematic liquid crystals have then been found to support bulk optical solitary waves[1,4], termed nematicons, and optical vortices[1,2,5]. A determining feature of nematic liquid crystals is their "nonlocal" response in that the response of the nematic medium to an optical forcing extends far beyond the waist of the optical beam[1,2,6]. This nonlocal response means that two or more nematic beams can interact at a distance via the nematic medium without the optical fields interacting directly. This strong nonlocal interaction results in the interaction between nematicons being attractive, independent of the relative phase

of the nematicons, as shown experimentally[7,8,9] and numerically[10], in contrast to local NLS solitons for which the interaction is attractive if the solitons are in-phase and repulsive if they are out of phase[11]. This attraction due to the nematic medium is strong enough to counteract the centrifugal repulsive force when two or more nematicons spiral around each other, so that a bound state can form[12,13,14,15], in analogy with gravitational attraction[14,15]. The mutual attraction between co-propagating nematicons, resulting in the formation of a bound state, also extends to counter-propagating nematicons[16,17,18]. Indeed, counter-propagating nematicons can merge to form a single beam on close enough approach[17,18].

One of the reasons for the experimental and theoretical interest in nonlinear optical beams in nematic liquid crystals is their possible application in all-optical devices[1]. An optical beam in a nematic liquid crystal can, in principle, be routed anywhere within a liquid crystal cell. It can then act as a reconfigurable "wire" for a co-propagated signal beam. In particular, a number of mechanisms have been proposed for nematicon-based logic gates and "light" valves, based on the controlled routing of a nematicon in a liquid crystal cell. The actual routing of the nematicon can be produced via a number of control mechanisms. The simplest is through an externally applied electric field[19]. The adjustment of this external electric field can be used to control the rotation of the nematic molecules, thus changing the refractive index of the nematic[1,20], resulting in refraction of the nematicon. Of interest to the current work, the trajectory of a nematicon can be controlled by the presence of another optical beam. This control beam can be in a plane orthogonal to the signal beam, resulting in a "light valve"[21,22], or can be a co-propagating nematicon in the same plane[7,23]. In particular, the control of a signal nematicon by a co-propagating control nematicon can be used to design power dependent X, NOR and AND logic gates[23].

The present work details a theoretical investigation of the control of the trajectory of a nematicon, the signal beam, by another co-propagating nematicon, the control beam, as in experimental investigations of nematicon-based logic gates[7,23]. This investigation will be based on the use of suitable trial functions for the nematicon solution in a Lagrangian formulation of the equations governing nonlinear optical beam propagation in nematic liquid crystals[24]. The use of trial functions is necessitated due to the lack of any exact solutions for a nematicon, except isolated solutions for fixed parameter values[25]. However, an appropriate choice of the trial function has been found to give approximate solutions in excellent agreement with full numerical solutions for a nematicon[2,24,25]. This holds for a range of trial functions, for example Gaussians and hyperbolic secants, as long as they are in broad agreement with numerical nematicon profiles. This approximate Lagrangian method has been previously used to study nematicon interaction[14,26,27], with excellent agreement found with numerical solutions.

In this study, the output position in a nematic cell of a signal beam (nematicon) will be controlled by another nematicon acting as a control beam. The input

positions of both beams are fixed, as well as the input angle of the signal beam. The output position of the signal beam is controlled by varying the input angle of the control beam. The input angle of the control beam required to lead to a specific output position of the signal beam is calculated. This input angle is calculated using both full numerical solutions of the nematicon equations and approximations based on the Lagrangian method discussed above. The first Lagrangian approach treats the beams as point particles, as their detailed profiles are averaged out, and yields dynamical equations for the beam trajectories which are analogous to those for point particles moving in a potential well which is determined by the response of the nematic medium. This particle approximation has been used in previous studies of interacting nematicons and has been found to yield excellent agreement with full numerical solutions[14,15]. In addition, these particle approximations have been found to be useful for general perturbed solitary wave problems[28]. However, in the present application to beam control this point particle approximation is found to yield only adequate agreement with full numerical solutions of the nematic equations, for reasons to be discussed. The particle approximation is then extended to take account of the detailed profile of the optical beams, yielding what is termed an extended particle approximation, but which could also be termed a rigid body approximation as the beam is now treated as an extended body. This extended Lagrangian approach is found to yield results in near perfect agreement with full numerical solutions, both for the beam trajectories and the input angle of the control beam required to obtain a given output position of the signal beam. This extension of the standard Lagrangian approach should prove useful for other problems involving solitary waves and their interactions and which have, to date, been studied using the standard particle approximation only[28].

2. Governing equations

Let us consider the propagation and incoherent interaction of two polarised beams of coherent light of the same wavelengths (colour) in a cell filled with a nematic liquid crystal. The electric fields of the beams are polarised in the same direction, which will be taken to be the x direction, with the z direction taken to be the propagation direction down the cell. The y direction then completes the coordinate triad. The cell will be taken to have a length D in the z direction. To overcome the Freédericksz threshold[20], the nematic molecules are initially at an angle θ_0 to the z direction. This pre-tilt can be produced, for instance, by an external low frequency electric field applied across the cell in the x direction. The cell and beam configuration are sketched in Figure 1. The electric fields of the optical beams then rotate the nematic molecules by the extra angle θ, so that the molecules make a total angle $\theta_0 + \theta$ to the z direction. In typical experiments the optical beams are of low, milliwatt power[1,2]. The extra rotation θ can then be assumed to be small, so that $|\theta| \ll \theta_0$. With this assumption, the non-dimensional equations governing the propagation of the optical beams through the liquid crystal cell in the slowly
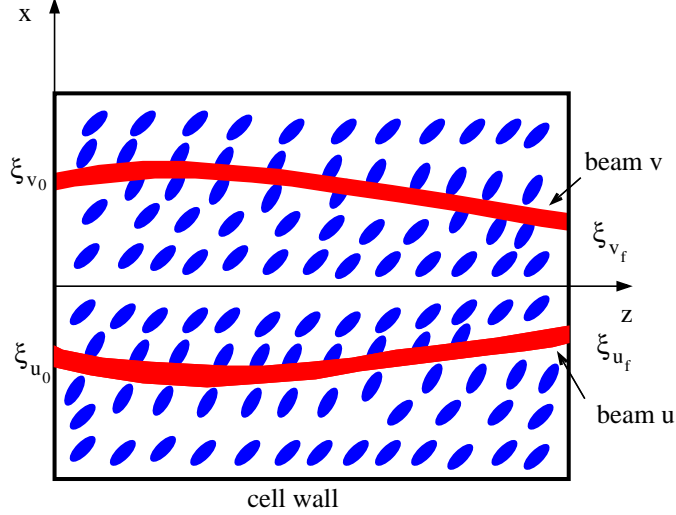
Fig. 1.   Schematic of liquid crystal cell showing the two interacting beams. The u and v beams are input at the angles U_{u_0} and U_{v_0}, respectively.

varying envelope, paraxial approximation[27,29] are

$$i\frac{\partial u}{\partial z} + \frac{1}{2}\nabla^2 u + 2\theta u = 0, \tag{2.1}$$

$$i\frac{\partial v}{\partial z} + \frac{1}{2}\nabla^2 v + 2\theta v = 0, \tag{2.2}$$

$$\nu\nabla^2\theta - 2q\theta = -2|u|^2 - 2|v|^2. \tag{2.3}$$

Here u and v are the electric field envelopes of the two optical beams. The parameter q is related to the pre-tilt. In the case of a pre-tilt produced by an external electric field it is proportional to the square of the amplitude of this field[4,6]. The elastic response of the nematic is measured by the parameter ν, which is $O(100)$ in the usual experimental regime[6,30,31]. As noted, due to the nonlocal response of the nematic, the beams do not have to overlap to interact, but can interact via the nematic response. As sketched in Figure 1 the u and v beams enter the cell at $x = \xi_{u_0}$ and $x = \xi_{v_0}$ at the angles $\alpha_{u0} = \tan^{-1} U_{u_0}$ and $\alpha_{v0} = \tan^{-1} U_{v_0}$ to the z direction and leave the cell at $x = \xi_{u_f}$ and $x = \xi_{v_f}$ at the angles $\alpha_{uf} = \tan^{-1} U_{u_f}$ and $\alpha_{vf} = \tan^{-1} U_{v_f}$ to the z direction, respectively. The beams' trajectories are altered due to their mutual interaction via the nematic. To greatly simplify the calculations, the cell will be taken to be much wider than the beams and the beams will be assumed to be launched near the centre of the cell. The effect of the boundaries can then be neglected and it can be assumed that $u \to 0$, $v \to 0$ and $\theta \to 0$ as $x^2 + y^2 \to \infty$. This is a reasonable assumption as typical beam widths are $3\mu m$ and typical cell widths are $75\mu m$[4].

While the system of equations (2.1)–(2.3) has been described for optical beams propagating in a nematic liquid crystal cell, the system is, in fact, general. It governs

nonlinear optical beam propagation in media for which nonlinearity is coupled to some diffusive phenomena[32], examples being thermal media[33], lead glasses[34,35,36] and certain photo-refractive crystals[37]. In addition, a similar system of equations arises in simplified α models of fluid turbulence[38,39].

3. Two body particle approximation

The two colour nematic equations (2.1)–(2.3) have the Lagrangian

$$
\begin{aligned}
L = {} & i\left(u^* u_z - u u_z^*\right) - |\nabla u|^2 + 4\theta|u|^2 + i\left(v^* v_z - v v_z^*\right) \\
& - |\nabla v|^2 + 4\theta|v|^2 - \nu|\nabla\theta|^2 - 2q\theta^2.
\end{aligned}
\tag{3.1}
$$

Lagrangian formulations of the nematic equations have been used to find approximate evolution equations for an evolving nematicon or nematicons[24,26,27], these equations being termed modulation equations[3]. Standard modulation theory[3] is based on the periodic wave or solitary wave solution of a nonlinear wave equation, which is taken to slowly vary so that its parameters, such as amplitude and width, are slowly varying functions of space (and time)[3,28]. However, even the equations for a single nematicon have no known general solitary wave solution, only isolated solutions for fixed values of the parameters q and ν[25]. To overcome this lack of an exact solution on which to base modulation theory, suitable trial functions are chosen for this unknown solution[40,41], which is then substituted into the Lagrangian formulation of the governing equations. Averaging the Lagrangian, that is integrating in x and y from $-\infty$ to ∞[3], then results in an averaged Lagrangian whose variational equations are the modulation equations for its varying parameters as a function of the evolution variable z. In the context of nonlinear beams in nematic liquid crystals, variational approximations have been found to give solutions in good agreement with experimental results[30,42,43] and numerical solutions[24,26,44,45,46,47].

Suitable trial functions to be used for this variational approximation for the two colour nematicon equations (2.1)–(2.3) are [24,27]

$$
u = a_u e^{-\chi_u^2/w_u^2}\, e^{i\psi_u},
\tag{3.2}
$$

$$
v = a_v e^{-\chi_v^2/w_v^2}\, e^{i\psi_v},
\tag{3.3}
$$

$$
\theta = \alpha_u e^{-2\chi_u^2/\beta_u^2} + \alpha_v e^{-2\chi_v^2/\beta_v^2},
\tag{3.4}
$$

where

$$
\chi_u = \sqrt{(x-\xi_u)^2 + y^2}, \quad \chi_v = \sqrt{(x-\xi_v)^2 + y^2},
$$
$$
\psi_u = \sigma_u + U_u\left(x - \xi_u\right), \quad \psi_v = \sigma_v + U_v\left(x - \xi_v\right).
\tag{3.5}
$$

The beam trial functions (3.2) and (3.3) are approximations to varying nematicons[24]. All the parameters of the trial functions (3.2)–(3.4) are usually taken to be functions of z[3,24,41]. However, it has been found that the amplitude-width

oscillations in a_u, w_u and a_v, w_v nearly decouple from the position-velocity oscillations in ξ_u, U_u and ξ_v, U_v[15,26,27,48,49,50,51,52]. The reduced modulation equations for the positions and velocities can then be obtained by assuming that the amplitudes a_u, a_v, α_u and α_v and widths w_u, w_v, β_u and β_v are constant, with only the positions ξ_u, ξ_v, velocities U_u, U_v and phases σ_u, σ_v depending on z. This approximation is the same as the particle approximation used for perturbed solitary wave theory[28].

As stated in Section 2, the nematic equations (2.1)–(2.3) are non-dimensional equations, with all quantities being made non-dimensional using typical dimensional beam parameters[30,31]. The beam widths are non-dimensionalised on a typical input width w_g of a Gaussian beam. A scale beam amplitude a_g is determined from the input power P_g of the Gaussian beam by[31]

$$P_g = \frac{\epsilon_0}{2} c n_o \int_{-\infty}^{\infty} \int_{-\infty}^{\infty} |u_g|^2 \, dx dy = \frac{\epsilon_0}{2} c n_o \frac{\pi}{2} a_g^2 w_g^2, \tag{3.6}$$

where c is the speed of light in a vacuum and n_o is the ordinary refractive index of the nematic medium. The non-dimensionalisation then depends on a typical input beam power, so that the parameters ν and q in the nematic equations (2.1)–(2.3) also depend on the scale input power. Of course, when the results are transformed back to dimensional variables, this dependence drops out[30,31]. For the numerical results of the present paper, the non-dimensional amplitudes and widths of the input beams used were $a_u = a_v = 2.0$ and $w_u = w_v = 4.1$. For typical $\nu = O(100)$[30,31], this gives that the ratios β_u/w_u and β_v/w_v are ~ 3, see equations (3.14) and (3.15) which determine β_u and β_v. We note that the amplitude and width of the director response are algebraically determined by the optical beam amplitudes and widths since the director equation (2.3) has no z derivatives. As the non-dimensional parameter ν controls the size of the ratios β_u/w_u and β_v/w_v, see (3.14) and (3.15), we refer to it as the "nonlocality," even though experimentally it is the relative sizes of β_u and β_v to the beam widths that measure the nonlocal response. The final physical parameter of interest is the pre-tilt θ_0. The actual value of this parameter is not needed for the solution of the non-dimensional equations (2.1)–(2.3). It only arises when the non-dimensional quantities are converted back to dimensional variables as it occurs in the definitions of ν and q[30,31].

Substituting the trial functions (3.2)–(3.4) into the Lagrangian (3.1) and averaging by integrating in x and y from $-\infty$ to ∞[3] results in the averaged Lagrangian

$$\begin{aligned}
\mathcal{L} = &-\pi a_u^2 w_u^2 \left(\sigma_u' - U_u \xi_u' \right) - \pi a_v^2 w_v^2 \left(\sigma_v' - U_v \xi_v' \right) - \pi a_u^2 - \pi a_v^2 \\
&+ 2\pi a_u^2 w_u^2 \alpha_u \beta_u^2 Q_1^{-1} - \frac{\pi}{2} a_u^2 w_u^2 U_u^2 - \frac{\pi}{2} a_v^2 w_v^2 U_v^2 - \pi \nu \alpha_u^2 - \pi \nu \alpha_v^2 \\
&- \frac{\pi}{2} q \alpha_u^2 \beta_u^2 - \frac{\pi}{2} q \alpha_v^2 \beta_v^2 + 2\pi a_v^2 w_v^2 \alpha_v \beta_v^2 Q_3^{-1} - \phi.
\end{aligned} \tag{3.7}$$

In this averaged Lagrangian, the interaction potential ϕ is

$$\begin{aligned}
\phi = &-2\pi a_u^2 w_u^2 \alpha_v \beta_v^2 Q_2^{-1} e^{-\gamma_1} - 2\pi a_v^2 w_v^2 \alpha_u \beta_u^2 Q_4^{-1} e^{-\gamma_2} \\
&+ 4\pi \nu \alpha_u \alpha_v \beta_u^2 \beta_v^2 Q_5^{-2} \left[1 - \gamma_3 \right] e^{-\gamma_3} + 2\pi q \alpha_u \alpha_v \beta_u^2 \beta_v^2 Q_5^{-1} e^{-\gamma_3}.
\end{aligned} \tag{3.8}$$

This potential will play a pivotal role in the analysis of the interaction of the two beams. In this averaged Lagrangian

$$Q_1 = \beta_u^2 + w_u^2, \quad Q_2 = \beta_v^2 + w_u^2, \quad Q_3 = \beta_v^2 + w_v^2,$$
$$Q_4 = \beta_u^2 + w_v^2, \quad Q_5 = \beta_u^2 + \beta_v^2, \tag{3.9}$$
$$\gamma_1 = \frac{2\rho^2}{Q_2}, \quad \gamma_2 = \frac{2\rho^2}{Q_4}, \quad \gamma_3 = \frac{2\rho^2}{Q_5}.$$

The distance ρ between the beams is

$$\rho = \xi_u - \xi_v. \tag{3.10}$$

To obtain the approximate equations governing the trajectories of the beams variations are taken of the averaged Lagrangian (3.7) with respect to the beams' position parameters. This results in the variational, or modulation[3], equations

$$\frac{1}{4}\left[\frac{d\sigma_u}{dz} - \frac{1}{2}U_u^2\right] = -\frac{1}{2}w_u^{-2} + \left[\alpha_u\beta_u^2\left(\beta_u^2 + w_u^2\right)Q_1^{-2}\right.$$
$$\left. + \alpha_v\beta_v^2\left(\beta_v^2 + w_u^2\right)Q_2^{-2}e^{-\gamma_1} - \alpha_v w_u^2\beta_v^2\rho^2 Q_2^{-3}e^{-\gamma_1}\right], \tag{3.11}$$

$$\frac{1}{4}a_u^2 w_u^2 \frac{dU_u}{dz} = -\frac{\partial\phi}{\partial\xi_u}, \tag{3.12}$$

$$\frac{d\xi_u}{dz} = U_u, \tag{3.13}$$

plus the algebraic equations

$$\left(\nu + \frac{1}{2}q\beta_u^2\right)\alpha_u - \beta_u^2\left(a_u^2 w_u^2 Q_1^{-1} + a_v^2 w_v^2 Q_4^{-1}e^{-\gamma_2}\right)$$
$$+ q\alpha_v\beta_u^2\beta_v^2 Q_5^{-1}e^{-\gamma_3} + 2\nu\alpha_v\beta_u^2\beta_v^2 Q_5^{-2}\left(1 - 2\rho^2 Q_5^{-1}\right)e^{-\gamma_3} = 0, \tag{3.14}$$

$$q\alpha_u - 4A_u a_u^2 w_u^4 Q_1^{-2} - 4A_v a_v^2 w_v^4 Q_4^{-2}e^{-\gamma_2} - 8A_v a_v^2 w_v^2\beta_u^2\rho^2 Q_4^{-3}e^{-\gamma_2}$$
$$+ 8\nu\alpha_v\beta_v^2 Q_5^{-3}\left[\beta_v^2 - \beta_u^2 - \left(\beta_v^2 - 3\beta_u^2\right)2\rho^2 Q_5^{-1} - 4\beta_u^2\rho^4 Q_5^{-2}\right]e^{-\gamma_3}$$
$$+ 4q\alpha_v\beta_v^2 Q_5^{-2}\left(\beta_v^2 + 2\beta_u^2\rho^2 Q_5^{-1}\right)e^{-\gamma_3} = 0, \tag{3.15}$$

for the nematicon parameters, together with symmetric equations for the v colour. Equation (3.11) for the phase σ_u of the nematicon, and its v colour equivalent, does not arise in the determination of the trajectories of the beams and will not be dealt with further. The amplitudes a_u, a_v and the widths w_u, w_v of the beams can be taken as their input values for the determination of these trajectories, as discussed above. The modulation equations (3.14) and (3.15), which are algebraic, and their v colour equivalents, then determine the corresponding amplitudes α_u and α_v and widths β_u and β_v of the director response.

The equations (3.12) and (3.13) for the positions of the nematicons, plus their v beam equivalents, can be reduced to dynamical equations for two mechanical particles under a central force whose potential is (3.8)[28]. In this analogy, ξ_u and ξ_v are the positions of the particles and U_u and U_v are their velocities. The modulation

equations (3.12) and (3.13) and their v equivalents then reduce to the mechanical system

$$M_u \frac{d^2 \xi_u}{dz^2} = -\frac{\partial \phi}{\partial \xi_u} = -\frac{\partial \phi}{\partial \rho},$$

$$M_v \frac{d^2 \xi_v}{dz^2} = -\frac{\partial \phi}{\partial \xi_v} = \frac{\partial \phi}{\partial \rho}. \tag{3.16}$$

The "masses" of the nematicons are

$$M_u = \frac{1}{4} a_u^2 w_u^2 \quad \text{and} \quad M_v = \frac{1}{4} a_v^2 w_v^2. \tag{3.17}$$

Physically, the masses M_u and M_v are the optical powers of the two beams. Unfortunately, the potential ϕ, (3.8), is not proportional to the masses, as in Newtonian gravitation. As the masses M_u and M_v cannot be divided out, further analysis is greatly simplified if the restriction to beams of equal initial masses, or equal optical powers, is taken, so that $M_u = M_v$.

For equal masses, the dynamical equations (3.16) have the centre of mass coordinate $\Xi_{cm} = \xi_u + \xi_v$. With this centre of mass coordinate, the particle equations (3.16) then transform to

$$\frac{d^2 \Xi_{cm}}{dz^2} = 0, \quad M_u \frac{d^2 \rho}{dz^2} = -2\frac{\partial \phi}{\partial \rho}. \tag{3.18}$$

The centre of mass has constant velocity, as expected, with the separation of the beams given by the second of (3.18). The centre of mass equation can now be integrated to give the momentum conservation result

$$\xi_u + \xi_v = (U_{u_0} + U_{v_0}) z + \xi_{u_0} + \xi_{v_0}, \tag{3.19}$$

since, as shown in Figure 1, the initial positions of the beams are $\xi_u = \xi_{u_0}$ and $\xi_v = \xi_{v_0}$ at $z = 0$. The separation equation, the second of (3.18), can be integrated to give the energy conservation equation

$$E = \frac{1}{2} M_u \dot{\rho}^2 + 2\phi(\rho), \tag{3.20}$$

with the energy E a constant. The separation of the beams is hence determined by

$$\int_{\xi_{u_0} - \xi_{v_0}}^{\rho} \frac{d\rho}{\sqrt{E - 2\phi(\rho)}} = \pm \sqrt{\frac{2}{M_u}}\, z. \tag{3.21}$$

Noting that the final positions of the beams are ξ_{u_f} and ξ_{v_f} at $z = D$ for the u and v beams, respectively, the momentum conservation result (3.19) gives the relation

$$U_{v_0} = \frac{1}{D} \left(\xi_{u_f} + \xi_{v_f} - \xi_{u_0} - \xi_{v_0} \right) - U_{u_0} \tag{3.22}$$

which links the positions of the input and output beams. In a similar manner, the energy conservation equation (3.21) gives another relation linking the input and

output beams

$$\int_{\xi_{u_0} - \xi_{v_0}}^{\xi_{u_f} - \xi_{v_f}} \frac{d\rho}{\sqrt{E - 2\phi(\rho)}} = \pm\sqrt{\frac{2}{M_u}}\, D. \qquad (3.23)$$

The $\pm$ sign is determined by whether $\xi_{u_f} - \xi_{v_f} > \xi_{u_0} - \xi_{v_0}$ or $\xi_{u_f} - \xi_{v_f} < \xi_{u_0} - \xi_{v_0}$. The two conservation equations (3.22) and (3.23) enable the input angle (velocity) U_{v_0} of the control beam v to be determined so that the signal beam u exits at a given ξ_{u_f}.

4. Extended particle approximation

The modulation equations developed so far have assumed that the optical beams can be approximated as point particles. However, as discussed in Section 5, the point particle modulation equations (3.16) give results which are in only adequate agreement with full numerical solutions of the nematic equations (2.1)–(2.3). This is because, as can be seen in Figures 3(a) and (b) and 5(a), that while the beams are initially well separated and have negligible overlap, especially in their tails, the beams can closely approach upon interaction. In these cases the point particle approximation underestimates the interaction between the nematicons and a better approximation is needed. This extra interaction in the tails was not important in previous studies of the interaction of nematicons as either the nematicons did not approach closely or the regions of closest approach were a minor part of their total interaction[14,26,27]. To get a more accurate estimate of the interaction potential between the beams their finite size must be taken into account.

The analogy of the previous section of the interaction of two optical beams and the interaction of two dynamical masses in a potential well can be further exploited to take account of the finite size of the beams. This is done using ideas and methods dating back to Newtonian gravitation to find the gravitational potential of finite masses with arbitrary density distributions. Let $\phi(x, y)$ be the potential for point masses and $P(x, y)$ be the density distribution of a general, finite mass. In the present analogy, $P(x, y)$ is the optical intensity distribution of a beam. Then the total potential Φ_{tot} due to the the finite mass is given by

$$\Phi_{tot} \iint_{-\infty}^{\infty} P(x, y)\, dxdy = \iint_{-\infty}^{\infty} P(x, y)\phi(x, y)\, dxdy. \qquad (4.1)$$

In the Newtonian gravitation analogy, P is the density distribution of the gravitating body and ϕ is the gravitational potential due to a point mass m_1, Gm_1/r. In the present case of optical beams the density is given by the trial functions (3.2) and (3.3), i.e. $\exp(-\chi_u^2/w_u^2)$ and $\exp(-\chi_v^2/w_v^2)$, and the potential is (3.8). The interaction potential between the two beams then contains three terms, (i) the interaction of a beam and the director distribution determined by the other beam (terms one and two in (3.8)), (ii) the interaction between the two parts of the director distribution forced by the two beams (term three containing the nonlocality ν in (3.8)),

which is related to the nonlocal effect of the liquid crystal, and (iii) the interaction between the two parts of the director distribution (term four in (3.8)), which is related to the applied field across the liquid crystal (i.e. q). Let us consider the contributions of each of these three terms in turn to the extended potential taking account of the finite size of the optical beams.

For the first contribution the beam u profile is $\exp(-\chi_u^2/w_u^2)$ and from (3.8) the point potential between a point on the beam (X_u, Y_u) and a general point (X_v, Y_v) on the director is then

$$ e^{-\frac{2[(X_u-X_v)^2+(Y_u-Y_v)^2]}{\beta_v^2+w_u^2}}. \tag{4.2} $$

We note that the width of this potential contribution has two contributions, the beam width w_u and the director response width β_v under the control beam. It was noted in Section 3 that $\beta_v \gg w_u$ as ν is large, $O(100)$, and the nematic response is highly nonlocal. This term could then be approximated by β_v^2 alone. However, the width contribution w_u^2 will be kept as the term (4.2) is then exact. The extended potential expression (4.1) therefore gives the corresponding potential contribution from a general point on the u beam over the entire width of the director distribution due to the other beam v as

$$ \frac{w_u^2 + \beta_v^2}{w_u^2 + 2\beta_v^2}\, e^{-\frac{2[(X_u-\xi_v)^2+(Y_u-\eta_v)^2]}{w_u^2+2\beta_v^2}}. \tag{4.3} $$

To calculate the effect of the finite width of the beam u the potential (4.1) is again used, but this time integrating over all points of the u beam. Taking a general point (X_u, Y_u) on the beam, the total potential contribution due to the finite beam u and the finite director response v is

$$ \Phi_{(i)} = \frac{w_u^2 + \beta_v^2}{w_u^2 + 2\beta_v^2} \frac{\iint\limits_{-\infty}^{\infty} e^{-\frac{2[(X_u-\xi_v)^2+(Y_u-\eta_v)^2]}{w_u^2+2\beta_v^2}} e^{-\frac{(X_u-\xi_u)^2+(Y_u-\eta_u)^2}{w_u^2}}\, dX_u dY_u}{\iint\limits_{-\infty}^{\infty} e^{-\frac{(X_u-\xi_u)^2+(Y_u-\eta_u)^2}{w_u^2}}\, dX_u dY_u}, \tag{4.4} $$

giving the result

$$ \Phi_{(i)}(\xi_u, \xi_v) = \frac{w_u^2 + \beta_v^2}{3w_u^2 + 2\beta_v^2} e^{-\frac{2\rho^2}{3w_u^2+2\beta_v^2}}. \tag{4.5} $$

The same reasoning can be applied to the interaction contributions (ii) and (iii), resulting in the separate potential contributions

$$ \Phi_{(ii)}(\xi_u, \xi_v) = \tfrac{1}{4}\left(1 - \frac{\rho^2}{\beta_u^2+\beta_v^2}\right) e^{-\frac{\rho^2}{\beta_u^2+\beta_v^2}}, \qquad (\nu) \tag{4.6} $$

$$ \Phi_{(iii)}(\xi_u, \xi_v) = \qquad \tfrac{1}{2} e^{-\frac{\rho^2}{\beta_u^2+\beta_v^2}}. \qquad (q) \tag{4.7} $$

Adding together the potential contributions (4.5)–(4.7) gives the total potential on treating the beams as extended objects as

$$ \Phi = -2\pi A_u a_u^2 w_u^2 \alpha_v \beta_v^2 Q_6^{-1} e^{-\gamma_5} - 2\pi A_v a_v^2 w_v^2 \alpha_u \beta_u^2 Q_7^{-1} e^{-\gamma_6} $$
$$ + \pi \nu \alpha_u \alpha_v \beta_u^2 \beta_v^2 Q_5^{-2} \left[1 - \gamma_4\right] e^{-\gamma_4} + \pi q \alpha_u \alpha_v \beta_u^2 \beta_v^2 Q_5^{-1} e^{-\gamma_4}. \tag{4.8} $$

Here

$$Q_6 = 2\beta_v^2 + 3w_u^2, \quad Q_7 = 2\beta_u^2 + 3w_v^2, \tag{4.9}$$

$$\gamma_4 = \frac{\rho^2}{Q_5}, \quad \gamma_5 = \frac{2\rho^2}{Q_6}, \quad \gamma_6 = \frac{\rho^2}{Q_7}.$$

The approximate equations for the trajectories of the beams based on this new, extended potential are (3.16) with ϕ replaced Φ.
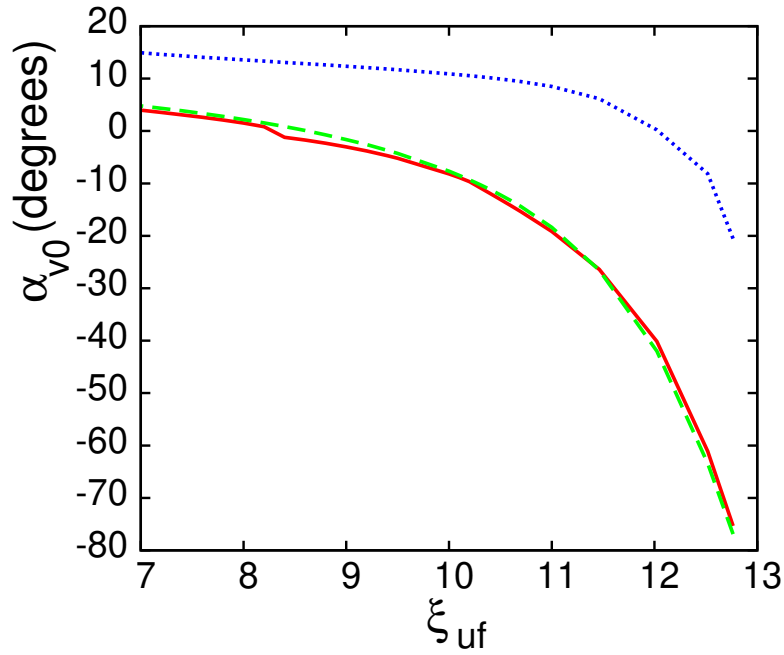

Fig. 2.   Input angle α_{v0} of control beam v needed to guide signal beam u to output position ξ_{uf}. The initial positions of the signal beam and the control beams are $\xi_{u0} = 13.0$ and $\xi_{v0} = -13.0$, respectively. Full numerical solution: dashed (green) line; particle approximation: dotted (blue) line; extended particle approximation: solid (red) line. Here $U_u = 0$, $\nu = 200$ and $D = 60$.

5. Results

The utility of the particle and extended particle modulation equations of Sections 3 and 4, respectively, will be demonstrated by comparing their predictions for the control parameter, the input angle U_{v_0} of the control beam v, so that the signal beam exits at a given point ξ_{u_f}, with the predictions of these two sets of equations with full numerical solutions of the nematicon equations (2.1)–(2.3). The modulation

equations (3.16) of Sections 3 and 4 were solved numerically using the standard 4th order Runge-Kutta scheme[53]. The NLS-type beam equations (2.1) and (2.2) were solved numerically using a pseudo-spectral method based on that of Fornberg and Whitham[54]. The director equation (2.3) was solved using a FFT based iterative method[26,53].

The system of equations (3.16) was solved as follows. Setting $M_u = M_v$ and making the substitutions

$$X = \xi_u - \xi_v$$
$$Y = \xi_u + \xi_v,$$

leads to the system of equations

$$M_u \frac{d^2 Y}{dz^2} = 0, \tag{5.1}$$

$$M_u \frac{d^2 X}{dz^2} = -2 \frac{\partial \phi}{\partial X}. \tag{5.2}$$

The centre of mass equation (5.1) has the solution

$$Y = k_1 z + k_2, \quad \text{where} \quad k_1 = V_{u_0} + V_{v_0} \quad \text{and} \quad k_2 = \xi_{u_0} + \xi_{v_0}.$$

Equation (5.2) for the difference in position of the beams leads to the differential equation

$$\dot{X} = \pm \sqrt{\frac{2}{M_u}(E - 2\phi(X))}, \tag{5.3}$$

where E is the total energy of the system and is a constant. The value of E is calculated from the initial kinetic and potential energies

$$E = \text{Kinetic energy} + \text{Potential energy}$$
$$= \frac{1}{2} M_u \dot{X}^2 + \phi(\xi_u, \xi_v)$$
$$= \frac{1}{2} M_u (U_{u_0} + U_{v_0})^2 + \phi(\xi_{u_0}, \xi_{v_0}).$$

The ordinary differential equation (5.3) was solved using the standard fourth order Runge-Kutta scheme[53]. For an initial velocity U_{v_0} of the control beam, the value of ξ_u for the signal beam was calculated at $z = D$. If the final value of ξ_u did not agree with the target value for the signal beam, the initial value of U_{v_0} for the control beam was then adjusted and the value of ξ_u at $z = D$ recalculated. This was done iteratively until the final position of the signal beam and the target value were sufficiently close, within 10^{-5}. To adjust the initial value of U_{v_0} a Lagrange interpolation polynomial between the target value of the signal beam and the initial velocity of the control beam was formed. The initial velocity that would set the polynomial to the target value was used[55]. The algebraic equations (3.14) and (3.15) were solved using steepest descents to obtain an initial guess and then Newton's method was used based on this initial guess[55].
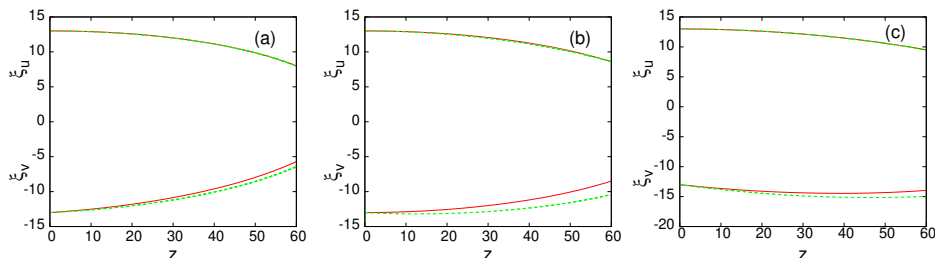
Fig. 3. Paths of signal and control beams as given by full numerical solutions of nematic equations (2.1)–(2.3) and the extended particle. Numerical trajectory: solid (red) line, u beam upper and v beam lower; extended particle approximation: dashed (green) line, u beam upper and v beam lower. The target positions of the signal beam are (a) $\xi_{uf} = 8.0$, (b) $\xi_{uf} = 8.6$, (c) $\xi_{uf} = 9.5$. Here $\xi_{u0} = 13$, $\xi_{v0} = -13$, $\nu = 200$ and $D = 60$.

The modulation theory predictions for the initial angle α_{v0} required for the signal beam to exit at $z = D$ at the position ξ_{uf} are compared with the numerical values in Figure 2. The initial positions of the beams are $\xi_{u0} = 13.0$ and $\xi_{v0} = -13.0$. The initial angle of the signal beam was $U_{u0} = 0$. The nonlocality was taken as $\nu = 200$ and the length of the cell was $D = 60$. It is clear that, as discussed above, the point particle approximation of Section 3 only yields basic agreement with the numerical results with the agreement becoming worse as the target position of the signal beam increases. As discussed in Section 4, the particle approximation predicts a control angle larger than the numerical value as it is based on an interaction between the beams which is too low. In contrast, the extended particle approximation of Section 4 gives excellent agreement with full numerical solutions over the full range of output positions. It should be noted that there is no angle α_{v0} which will route the signal beam to a position $\xi_{uf} > 13.0$. The output position of the signal beam is then not arbitrarily adjustable.

The agreement between the detailed beam trajectories as given by full numerical solutions of the nematic equations (2.1)–(2.3) and the extended modulation theory of Section 4 is shown in Figure 3. Based on the agreement shown in Figure 2 the trajectories of the particle approximation of Section 3 are not shown. Figure 3 shows the trajectory comparisons for both the signal u and control beams v for a range of output positions ξ_{uf} of the signal beam. As for the comparisons of Figure 2 the predictions of the extended particle model are in excellent agreement with the numerical solutions. The approximate trajectories for the signal beam u are identical with the numerical trajectories. This is expected as this trajectory is highly constrained as its start point ξ_{u0} and end point ξ_{uf} are fixed. In contrast, the end point ξ_{vf} of the control beam is free. Even with this freedom, the approximate trajectory for the control beam v is in excellent agreement with the numerical trajectory.

Figure 4 shows a similar comparison as for Figure 2 for the control beam angle
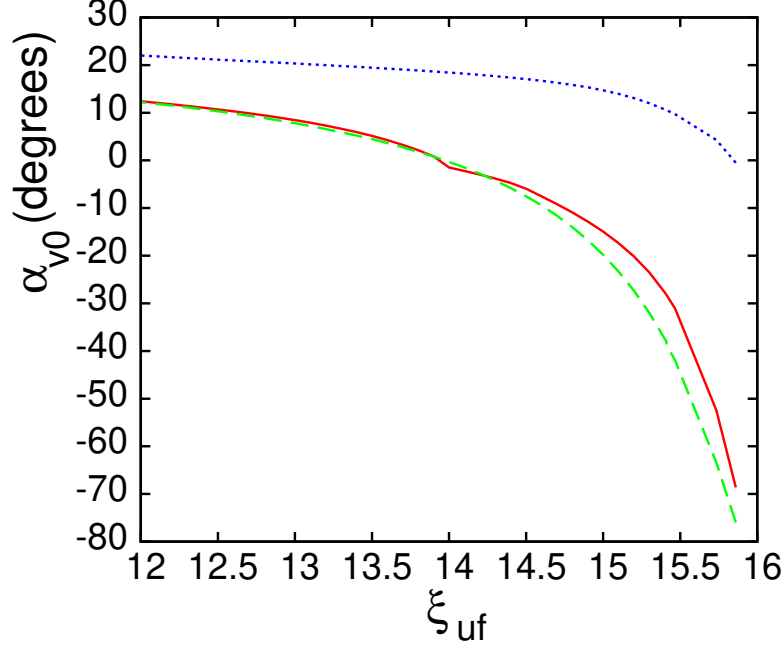
Fig. 4.   Input angle α_{v0} of control beam v needed to guide signal beam u to output position ξ_{uf}. The initial positions of the signal beam and the control beams are $\xi_{u0} = 16.0$ and $\xi_{v0} = -16.0$, respectively. Full numerical solution: dashed (green) line; particle approximation: dotted (blue) line; extended particle approximation: solid (red) line. Here $U_{u0} = 0$, $\nu = 225$ and $D = 60$.

α_{v0} to route the signal beam to the output position ξ_{uf}. The beams are input further apart with $\xi_{u0} = 16$ and $\xi_{v0} = -16$ and the nonlocality is slightly higher with $\nu = 225$. The length $D = 60$ of the cell is the same. The conclusions from this new comparison are the same as those for Figure 2. The particle approximation of Section 3 only gives adequate agreement with the numerical results, again due to the interaction between the beams on which the approximation is made being too low due to treating the beams as point particles, rather than extended bodies. In contrast, the extended particle approximation of Section 4 gives an excellent comparison with the numerical results. This is again due to it taking account of the beams being extended bodies, not point particles. The control angles α_{v0} needed to route the beam are larger than those of Figure 2 as the increased separation means that the interaction between the beams is lower. As for Figure 2 there is a maximum deflection of the signal beam and it is not possible to find a control angle α_{v0} to route the signal beam to $\xi_{uf} > 16$.

Figure 5 shows detailed individual beam trajectory comparisons for three of the cases of Figure 4. These results are very similar to the equivalent results of Figure
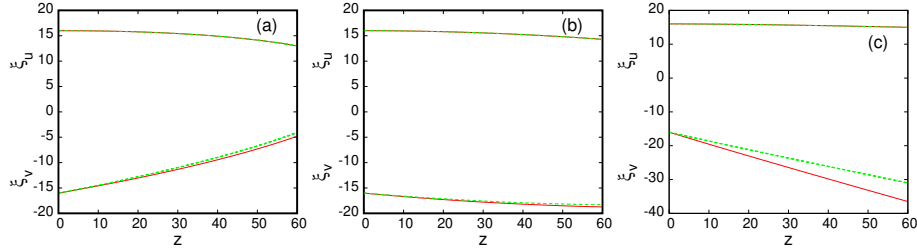
Fig. 5. Paths of signal and control beams as given by full numerical solutions of nematic equations (2.1)–(2.3) and the extended particle. Numerical trajectory: solid (red) line, u beam upper and v beam lower; extended particle approximation: dashed (green) line, u beam upper and v beam lower. The target positions of the signal beam are (a) $\xi_{uf} = 13.0$, (b) $\xi_{uf} = 14.3$, (c) $\xi_{uf} = 15.0$. Here $U_{u0} = 0$, $\nu = 225$ and $D = 60$.

3. The agreement of the signal beam trajectory as given by the extended particle modulation theory is in perfect agreement with the numerical results. This is due to this signal trajectory being constrained at its start and end points. This means that the trajectory between these points has little scope for variation. The extended particle modulation analysis control beam trajectories are in excellent agreement with the numerical trajectories, with some disagreement for higher values of the exit point ξ_{uf} of the signal beam. In general, as can be seen from Figures 3 and 5, the smaller the overlap between the control and signal beams, the greater the difference between the numerical and particle approximation control beam trajectories. This is because as the interaction becomes (exponentially) weaker, the more significant are small errors in the particle approximation.

6. Conclusions

Modulation theory based on averaged Lagrangians has been found to give excellent results for the interaction of two nonlinear optical beams in a nematic liquid crystal cell. This interaction is used as a model for an all-optical device which uses a control beam to route a signal beam to a given output position at the end of the cell. It is found that standard modulation theory which treats the beams as point particles does not perform well in predicting the input angle of the control beam, the control parameter, even though this modulation theory has performed well in previous studies of nematicon interaction[14,26,27]. An extended modulation theory which takes account of the extended profile of the beams is found to give results in excellent agreement with full numerical solutions. This extended theory is based on that used in Newtonian gravitation to find the interaction of two finite size masses with arbitrary density distributions. It is expected that a similar extended analysis will be useful to give simple, accurate approximations for other studies of solitary wave interaction. To this end, the extended particle approach is expected to have a wider range of validity than the point particle approximation as it can

more accurately model the interaction of solitary waves when they have significant overlap.

The particle model makes it easy to understand the forces that are operating between optical beams in liquid crystals. Such models also give information as to the physics of the underlying interaction. They also allow fast predictions of the interaction as they are based on ordinary, rather than partial, differential equations. The model can only produce reliable predictions when the optical beams can be treated as indivisible particles. If the power of a beam is too low, then it will not form a solitary wave. On the other hand, if it is too high, then the beam will break up into multiple solitary waves. In both these situations, the particle method will not produce reliable results and cannot be used without further extensions.

References

1. M. Peccianti and G. Assanto, "Nematicons," *Phys. Rep.,* **516**, 147–208 (2012).
2. G. Assanto, *Nematicons, spatial optical solitons in nematic liquid crystals,* John Wiley and Sons, New York (2012).
3. G.B. Whitham, *Linear and Nonlinear Waves,* J. Wiley and Sons, New York (1974).
4. M. Peccianti, A. de Rossi, G. Assanto, A. De Luca, C. Umeton and I.C. Khoo, "Electrically assisted self-confinement and waveguiding in planar nematic liquid crystal cells," *Appl. Phys. Lett.,* **77**, 7–9 (2000).
5. Y.V. Izdebskaya, J. Rebling, A.S. Desyatnikov and Y.S. Kivshar, "Observation of vector solitons with hidden vorticity," *Opt. Lett.,* **37**, 767–769 (2012).
6. C. Conti, M. Peccianti and G. Assanto, "Route to nonlocality and observation of accessible solitons," *Phys. Rev. Lett.,* **91**, 073901 (2003).
7. M. Peccianti, K.A. Brzdąkiewicz and G. Assanto, "Nonlocal spatial soliton interactions in nematic liquid crystals," *Opt. Lett.,* **27**, 1460–1462 (2002).
8. G. Assanto and M. Peccianti, "Spatial solitons in nematic liquid crystals," *IEEE J. Quantum Electron.,* **39**, 13–21 (2003).
9. G. Assanto, M. Peccianti, K.A. Brzdąiewicz, A. de Luca and C. Umeton, "Nonlinear wave propagation and spatial solitons in nematic liquid crystals," *J. Nonlinear Opt. Phys. Mater.,* **12**, 123–134 (2003).
10. W. Hu, T. Zhang, Q. Guo, L. Xuan and S. Lan, "Nonlocality-controlled interaction of spatial solitons in nematic liquid crystals," *Appl. Phys. Lett.,* **89**, 071111 (2006).
11. Y.S. Kivshar and G.P. Agrawal, *Optical Solitons. From Fibers to Photonic Crystals,* Academic Press, San Diego (2003).
12. A. Fratalocchi, A. Piccardi, M. Peccianti and G. Assanto, Nonlinear management of the angular momentum of soliton clusters: Theory and experiments," *Phys. Rev. Lett.,* **75**, 063835 (2007).
13. A. Fratalocchi, M. Peccianti, C. Conti and G. Assanto, "Spiraling and cyclic dynamics of nematicons," *Mol. Cryst. Liq. Cryst.,* **421** 197–207 (2004).
14. G. Assanto, N.F. Smyth and A.L. Worthy, "Two colour, nonlocal vector solitary waves with angular momentum in nematic liquid crystals," *Phys. Rev. A,* **78**, 013832 (2008).
15. G. Assanto, C. García-Reimbert, A.A. Minzoni, N.F. Smyth, and A.L. Worthy, "Lagrange solution for three wavelength solitary wave clusters in nematic liquid crystals," *Physica D,* **240**, 1213–1219 (2011).
16. J.F. Henninot, M. Debailleul, M. Warenghem, "Tunable non-locality of thermal non-

linearity in dye doped nematic liquid crystal," *Mol. Cryst. Liq. Cryst.,* **375**, 631–640 (2002).

17. J.F. Henninot, J.F. Blach and M. Warenghem, "Experimental study of the nonlocality of spatial optical solitons excited in nematic liquid crystal," *J. Opt. A: Pure Appl. Opt.,* **9**, 20–25 (2007).

18. Y.V. Izdebskaya, V.G. Shvedov, A.S. Desyatnikov, W.Z. Krolikowski, Milivoj Belić, G. Assanto and Y.S. Kivshar, "Counterpropagating nematicons in bias-free liquid crystals," *Opt. Express,* **18**, 3258–3263 (2010).

19. M. Peccianti, C. Conti, G. Assanto, A. De Luca and C. Umeton, "Routing of anisotropic spatial solitons and modulational instability in liquid crystals," *Nature,* **432**, 733–737 (2004).

20. I.C. Khoo, *Liquid Crystals: Physical Properties and Nonlinear Optical Phenomena,* Wiley, New York (1995).

21. S.V. Serak, N.V. Tabiryan, M. Peccianti and G. Assanto, "Spatial soliton all-optical logic gates," *IEEE Photon. Tech. Lett.,* **18**, 1287–1289 (2006).

22. A. Piccardi, A. Alberucci, U. Bortolozzo, S. Residori and G. Assanto, "Soliton gating and switching in liquid crystal light valve," *Appl. Phys. Lett.,* **96**, 071104 (2010).

23. M. Peccianti, C. Conti, G. Assanto, A. De Luca and C. Umeton, "All-optical switching and logic gating with spatial solitons in liquid crystals," *Appl. Phys. Lett.,* **81**, 3335–3337 (2002).

24. A.A. Minzoni, N.F. Smyth and A.L. Worthy, "Modulation solutions for nematicon propagation in non-local liquid crystals," *J. Opt. Soc. Amer. B,* **24**, 1549–1556 (2007).

25. J.M.L. MacNeil, N.F. Smyth and G. Assanto, "Exact and approximate solutions for solitary waves in nematic liquid crystals," *Physica D,* **284**, 1–15 (2014).

26. B.D. Skuse and N.F. Smyth, "Two-colour vector soliton interactions in nematic liquid crystals in the local response regime," *Phys. Rev. A*, **77**, 013817 (2008).

27. B.D. Skuse and N.F. Smyth, "Interaction of two colour solitary waves in a liquid crystal in the nonlocal regime," *Phys. Rev. A,* **79**, 063806 (2009).

28. D.J. Kaup and A.C. Newell, "Solitons as particles, oscillators, and in slowly changing media: a singular perturbation theory," *Proc. Roy. Soc. Lond. A 361,* 413–446 (1978).

29. A. Alberucci, M. Peccianti, G. Assanto, A. Dyadyusha and M. Kaczmarek, "Two-color vector solitons in nonlocal media," *Phys. Rev. Lett. 97,* 153903 (2006).

30. G. Assanto, A.A. Minzoni, M. Peccianti and N.F. Smyth, "Optical solitary waves escaping a wide trapping potential in nematic liquid crystals: modulation theory," *Phys. Rev. A,* **79**, 033837 (2009).

31. Y. Izdebskaya, W. Krolikowski, N.F. Smyth and G. Assanto, "Vortex stabilization by means of spatial solitons in nonlocal media," *J. Opt.,* **18**, 054006 (2016).

32. A.B. Aceves, J.V. Moloney and A.C. Newell, "Theory of light-beam propagation at nonlinear interfaces. I Equivalent-particle theory for a single interface," *Phys. Rev. A,* **39**, 1809–1827 (1989).

33. E.A. Kuznetsov and A.M. Rubenchik, "Soliton stabilization in plasmas and hydrodynamics," *Phys. Reports*, **142**, 103–165 (1986).

34. F.W. Dabby and J.R. Whinnery, "Thermal self-focusing of laser beams in lead glasses," *Appl. Phys. Lett.,* **13**, 284–286 (1968).

35. C. Rotschild, M. Segev, Z. Xu, Y.V. Kartashov and L. Torner, "Two-dimensional multipole solitons in nonlocal nonlinear media," *Opt. Lett.,* **31**, 3312–3314 (2006).

36. C. Rotschild, B. Alfassi, O. Cohen and M. Segev, "Long-range interactions between optical solitons," *Nature Phys.,* **2**, 769–774 (2006).

37. M. Segev, B. Crosignani, A. Yariv and B. Fischer, "Spatial solitons in photorefractive media," *Phys. Rev. Lett.,* **68**, 923–926 (1992).

38. A. Cheskidov, D.D. Holm, E. Olson and E.S. Titi, "On a Leray-α model of turbulence," *Proc. R. Soc. Lond. A*, **461**, 629–649 (2005).
39. A. Ilyin, E.M. Lunasin and E.S. Titi, "A modified-Leray-α subgrid scale model of turbulence," *Nonlinearity*, **19**, 879–897 (2006).
40. B. Malomed, "Variational methods in nonlinear fiber optics and related fields," *Prog. Opt.*, **43**, 71–193 (2002).
41. W.L. Kath and N.F. Smyth, "Soliton evolution and radiation loss for the nonlinear Schrodinger equation," *Phys. Rev. E*, **51**, 1484–1492 (1995).
42. G. Assanto, N.F. Smyth and W. Xia, "Modulation analysis of nonlinear beam refraction at an interface in liquid crystals," *Phys. Rev. A*, **84**, 033818 (2011).
43. G. Assanto, N.F. Smyth and W. Xia, "Refraction of nonlinear light beams in nematic liquid crystals," *J. Nonlin. Opt. Phys. Mater.*, **21**, 1250033 (2012).
44. A.A. Minzoni, N.F. Smyth, A.L. Worthy and Y.S. Kivshar, "Stabilization of vortex solitons in nonlocal nonlinear media," *Phys. Rev. A*, **76**, 063803 (2007).
45. A.A. Minzoni, N.F. Smyth and Z. Xu, "Stability of an optical vortex in a circular nematic cell," *Phys. Rev. A*, **81**, 033816 (2010).
46. N.F. Smyth and W. Xia, "Refraction and instability of optical vortices at an interface in a liquid crystal," *J. Phys. B: At. Mol. Opt. Phys.*, **45**, 165403 (2012).
47. G. Assanto, A.A. Minzoni, N.F. Smyth and A.L. Worthy, "Refraction of nonlinear beams by localised refractive index changes in nematic liquid crystals," *Phys. Rev. A*, **82**, 053843 (2010).
48. G. Assanto, B.D. Skuse and N.F. Smyth, "Solitary wave propagation and steering through light-induced refractive potentials," *Phys. Rev. A,* **81**, 063811 (2010).
49. G. Assanto, A.A. Minzoni, N.F. Smyth and A.L. Worthy, "Refraction of nonlinear beams by localised refractive index changes in nematic liquid crystals," *Phys. Rev. A,* **82**, 053843 (2010).
50. A. Alberucci, G. Assanto, A.A. Minzoni and N.F. Smyth, "Scattering of reorientational optical solitary waves at dielectric perturbations," *Phys. Rev. A,* **85**, 013804 (2012).
51. G. Assanto, A.A. Minzoni and N.F. Smyth, "Vortex confinement and bending with nonlocal solitons," *Opt. Lett.,* **39**, 509–512 (2014).
52. G. Assanto, A.A. Minzoni and N.F. Smyth, "Deflection of nematicon-vortex vector solitons in liquid crystals," *Phys. Rev. A,* **89**, 013827 (2014).
53. W.H. Press, S.A. Teukolsky, W.T. Vetterling, and B.P. Flannery, *Numerical Recipes in Fortran. The Art of Scientific Computing,* Cambridge University Press (1992).
54. B. Fornberg and G.B. Whitham, "A numerical and theoretical study of certain nonlinear wave phenomena," *Phil. Trans. Roy. Soc. London A 289*, 373–403 (1978).
55. R. Burden and J. Faires, *Numerical Analysis,* Brookes/Cole, Boston, Massachusetts (2011).